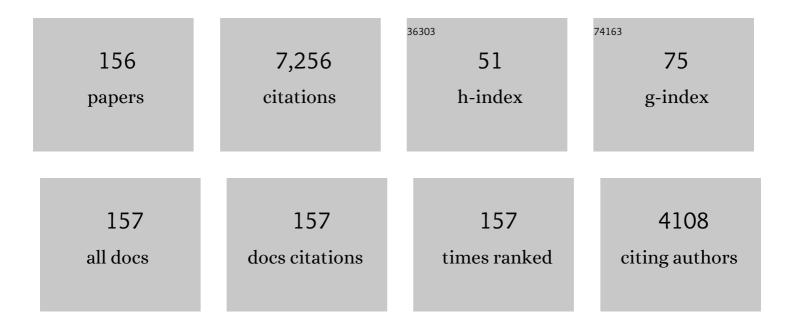
List of Publications by Year in descending order

Source: https://exaly.com/author-pdf/8400501/publications.pdf Version: 2024-02-01



Υιέιι Ζηλνις

#	Article	IF	CITATIONS
1	Designed mesoporous hollow sphere architecture metal (Mn, Co, Ni) silicate: A potential electrode material for flexible all solid-state asymmetric supercapacitor. Chemical Engineering Journal, 2019, 362, 818-829.	12.7	225
2	Fast and reversible zinc ion intercalation in Al-ion modified hydrated vanadate. Nano Energy, 2020, 70, 104519.	16.0	188
3	Stitching of Zn <sub>3</sub> (OH) <sub>2</sub> V <sub>2</sub> O <sub>7</sub> ·2H <sub>2</sub> O 2D Nanosheets by 1D Carbon Nanotubes Boosts Ultrahigh Rate for Wearable Quasi-Solid-State Zinc-Ion Batteries. ACS Nano, 2020, 14, 842-853.	14.6	183
4	Hydrothermal encapsulation of VO <sub>2</sub> (A) nanorods in amorphous carbon by carbonization of glucose for energy storage devices. Dalton Transactions, 2018, 47, 452-464.	3.3	171
5	Cobalt-nickel silicate hydroxide on amorphous carbon derived from bamboo leaves for hybrid supercapacitors. Chemical Engineering Journal, 2019, 375, 121938.	12.7	171
6	Fabrication of (NH4)2V3O8 nanoparticles encapsulated in amorphous carbon for high capacity electrodes in aqueous zinc ion batteries. Chemical Engineering Journal, 2020, 382, 122844.	12.7	164
7	In-situ grown manganese silicate from biomass-derived heteroatom-doped porous carbon for supercapacitors with high performance. Journal of Colloid and Interface Science, 2019, 534, 142-155.	9.4	146
8	In-situ hydrothermal growth of Zn4Si2O7(OH)2·H2O anchored on 3D N, S-enriched carbon derived from plant biomass for flexible solid-state asymmetrical supercapacitors. Chemical Engineering Journal, 2018, 352, 519-529.	12.7	143
9	Fabrication of V 2 O 5 with various morphologies for high-performance electrochemical capacitor. Applied Surface Science, 2016, 377, 385-393.	6.1	121
10	Facile hydrothermal synthesis of ultrahigh-aspect-ratio V2O5 nanowires for high-performance supercapacitors. Current Applied Physics, 2015, 15, 493-498.	2.4	110
11	In Situ Generated Ni <sub>3</sub> Si <sub>2</sub> O <sub>5</sub> (OH) <sub>4</sub> on Mesoporous Heteroatom-Enriched Carbon Derived from Natural Bamboo Leaves for High-Performance Supercapacitors. ACS Applied Energy Materials, 2018, 1, 3396-3409.	5.1	109
12	Ammonium Vanadium Oxide [(NH <sub>4</sub> ) <sub>2</sub> V <sub>4</sub> O <sub>9</sub> ] Sheets for High Capacity Electrodes in Aqueous Zinc Ion Batteries. ACS Applied Energy Materials, 2019, 2, 7861-7869.	5.1	107
13	Improve the catalytic activity of $\hat{l}\pm$ -Fe2O3 particles in decomposition of ammonium perchlorate by coating amorphous carbon on their surface. Journal of Solid State Chemistry, 2011, 184, 387-390.	2.9	102
14	Kelp-derived three-dimensional hierarchical porous N, O-doped carbon for flexible solid-state symmetrical supercapacitors with excellent performance. Applied Surface Science, 2018, 447, 876-885.	6.1	102
15	Beltlike V <sub>2</sub> O <sub>3</sub> @C Core–Shellâ€Structured Composite: Design, Preparation, Characterization, Phase Transition, and Improvement of Electrochemical Properties of V <sub>2</sub> O <sub>3</sub> . European Journal of Inorganic Chemistry, 2012, 2012, 1650-1659.	2.0	100
16	All-in-one stretchable coaxial-fiber strain sensor integrated with high-performing supercapacitor. Energy Storage Materials, 2020, 25, 124-130.	18.0	100
17	Facile fabrication of Fe3O4 and Co3O4 microspheres and their influence on the thermal decomposition of ammonium perchlorate. Journal of Alloys and Compounds, 2016, 674, 259-265.	5.5	96
18	Template Fabrication of Amorphous Co <sub>2</sub> SiO <sub>4</sub> Nanobelts/Graphene Oxide Composites with Enhanced Electrochemical Performances for Hybrid Supercapacitors. ACS Applied Energy Materials, 2019, 2, 3830-3839.	5.1	96

#	Article	IF	CITATIONS
19	<i>In situ</i> grown 2D hydrated ammonium vanadate nanosheets on carbon cloth as a free-standing cathode for high-performance rechargeable Zn-ion batteries. Journal of Materials Chemistry A, 2020, 8, 15130-15139.	10.3	91
20	Synthesis and supercapacitor electrode of VO2(B)/C core–shell composites with a pseudocapacitance in aqueous solution. Applied Surface Science, 2016, 371, 189-195.	6.1	90
21	3D hierarchical porous V3O7·H2O nanobelts/CNT/reduced graphene oxide integrated composite with synergistic effect for supercapacitors with high capacitance and long cycling life. Journal of Colloid and Interface Science, 2018, 531, 382-393.	9.4	90
22	New Strategy for the Morphology-Controlled Synthesis of V <sub>2</sub> O <sub>5</sub> Microcrystals with Enhanced Capacitance as Battery-type Supercapacitor Electrodes. Crystal Growth and Design, 2018, 18, 5365-5376.	3.0	88
23	Dual ions enable vanadium oxide hydration with superior Zn2+ storage for aqueous zinc-ion batteries. Chemical Engineering Journal, 2022, 433, 133795.	12.7	88
24	Three-dimensional porous V <sub>2</sub> O <sub>5</sub> hierarchical spheres as a battery-type electrode for a hybrid supercapacitor with excellent charge storage performance. Dalton Transactions, 2017, 46, 15048-15058.	3.3	87
25	Single-Atom Catalysts: Advances and Challenges in Metal-Support Interactions for Enhanced Electrocatalysis. Electrochemical Energy Reviews, 2022, 5, 145-186.	25.5	86
26	Controlled synthesis of 3D porous VO <sub>2</sub> (B) hierarchical spheres with different interiors for energy storage. Inorganic Chemistry Frontiers, 2018, 5, 2798-2810.	6.0	85
27	Hydrothermal synthesis, characterization, formation mechanism and electrochemical property of V3O7·H2O single-crystal nanobelts. Materials Science and Engineering B: Solid-State Materials for Advanced Technology, 2010, 175, 164-171.	3.5	84
28	Sandwich-like honeycomb Co2SiO4/rGO/honeycomb Co2SiO4 structures with enhanced electrochemical properties for high-performance hybrid supercapacitor. Journal of Power Sources, 2021, 492, 229643.	7.8	84
29	3D Interlaced Networks of VO(OH) <sub>2</sub> Nanoflakes Wrapped with Graphene Oxide Nanosheets as Electrodes for Energy Storage Devices. ACS Applied Nano Materials, 2019, 2, 2934-2945.	5.0	83
30	Coupled cobalt silicate nanobelt-on-nanobelt hierarchy structure with reduced graphene oxide for enhanced supercapacitive performance. Journal of Power Sources, 2020, 448, 227407.	7.8	82
31	NH <sub>4</sub> V <sub>3</sub> O <sub>8</sub> ·0.5H <sub>2</sub> O nanobelts with intercalated water molecules as a high performance zinc ion battery cathode. Materials Chemistry Frontiers, 2020, 4, 1434-1443.	5.9	81
32	Copper oxide/cuprous oxide/hierarchical porous biomass-derived carbon hybrid composites for high-performance supercapacitor electrode. Journal of Alloys and Compounds, 2019, 782, 1103-1113.	5.5	78
33	Ammonium ion intercalated hydrated vanadium pentoxide for advanced aqueous rechargeable Zn-ion batteries. Materials Today Energy, 2020, 18, 100509.	4.7	77
34	A facile method for preparing VO2 nanobelts. Materials Letters, 2008, 62, 1878-1880.	2.6	76
35	A novel ordered hollow spherical nickel silicate–nickel hydroxide composite with two types of morphologies for enhanced electrochemical storage performance. Materials Chemistry Frontiers, 2019, 3, 2090-2101.	5.9	74
36	Alkali etching metal silicates derived from bamboo leaves with enhanced electrochemical properties for solid-state hybrid supercapacitors. Chemical Engineering Journal, 2021, 417, 127964.	12.7	73

#	Article	IF	CITATIONS
37	Facile hydrothermal synthesis of vanadium oxides nanobelts by ethanol reduction of peroxovanadium complexes. Ceramics International, 2013, 39, 129-141.	4.8	72
38	Fabrication of vanadium sulfide (VS4) wrapped with carbonaceous materials as an enhanced electrode for symmetric supercapacitors. Journal of Colloid and Interface Science, 2020, 574, 312-323.	9.4	71
39	Facile hydrothermal synthesis and electrochemical properties of (NH4)2V10O25·8H2O nanobelts for high-performance aqueous zinc ion batteries. Electrochimica Acta, 2020, 332, 135506.	5.2	67
40	One-step hydrothermal preparation of (NH4)2V3O8/carbon composites and conversion to porous V2O5 nanoparticles as supercapacitor electrode with excellent pseudocapacitive capability. Applied Surface Science, 2017, 423, 728-742.	6.1	60
41	"Double guarantee mechanism―of Ca <sup>2+</sup> -intercalation and rGO-integration ensures hydrated vanadium oxide with high performance for aqueous zinc-ion batteries. Inorganic Chemistry Frontiers, 2021, 8, 79-89.	6.0	59
42	Hydrothermal synthesis of VS4/CNTs composite with petal-shape structures performing a high specific capacity in a large potential range for high-performance symmetric supercapacitors. Journal of Colloid and Interface Science, 2019, 554, 191-201.	9.4	57
43	Polyaniline-expanded the interlayer spacing of hydrated vanadium pentoxide by the interface-intercalation for aqueous rechargeable Zn-ion batteries. Journal of Colloid and Interface Science, 2021, 603, 641-650.	9.4	57
44	Rice husk-derived Mn <sub>3</sub> O <sub>4</sub> /manganese silicate/C nanostructured composites for high-performance hybrid supercapacitors. Inorganic Chemistry Frontiers, 2019, 6, 2788-2800.	6.0	56
45	Hydrated vanadium pentoxide/reduced graphene oxide-polyvinyl alcohol (V2O5â‹nH2O/rGO-PVA) film as a binder-free electrode for solid-state Zn-ion batteries. Journal of Colloid and Interface Science, 2021, 587, 845-854.	9.4	56
46	Fabrication of V3O7·H2O@C core-shell nanostructured composites and the effect of V3O7·H2O and V3O7·H2O@C on decomposition of ammonium perchlorate. Journal of Alloys and Compounds, 2011, 509, L69-L73.	5.5	55
47	Preparation of W- and Mo-doped VO2(M) by ethanol reduction of peroxovanadium complexes and their phase transition and optical switching properties. Journal of Alloys and Compounds, 2012, 544, 30-36.	5.5	55
48	A strategy for the synthesis of VN@C and VC@C core–shell composites with hierarchically porous structures and large specific surface areas for high performance symmetric supercapacitors. Dalton Transactions, 2018, 47, 8052-8062.	3.3	55
49	Hydrothermal synthesis of vanadium dioxides/carbon composites and their transformation to surface-uneven V <sub>2</sub> O <sub>5</sub> nanoparticles with high electrochemical properties. RSC Advances, 2016, 6, 93741-93752.	3.6	54
50	Facile preparation, optical and electrochemical properties of layer-by-layer V 2 O 5 quadrate structures. Applied Surface Science, 2017, 399, 151-159.	6.1	54
51	Synthesis of amorphous cobalt silicate nanobelts@manganese silicate core–shell structures as enhanced electrode for high-performance hybrid supercapacitors. Journal of Colloid and Interface Science, 2020, 561, 762-771.	9.4	52
52	V2O3/C nanocomposites with interface defects for enhanced intercalation pseudocapacitance. Electrochimica Acta, 2019, 318, 635-643.	5.2	51
53	Improvement of the electrochemical properties of V3O7·H2O nanobelts for Li battery application through synthesis of V3O7@C core-shell nanostructured composites. Current Applied Physics, 2011, 11, 1159-1163.	2.4	50
54	The additives W, Mo, Sn and Fe for promoting the formation of VO2(M) and its optical switching properties. Materials Letters, 2013, 92, 61-64.	2.6	49

#	Article	IF	CITATIONS
55	Direct preparation and formation mechanism of belt-like doped VO2(M) with rectangular cross sections by one-step hydrothermal route and their phase transition and optical switching properties. Journal of Alloys and Compounds, 2013, 570, 104-113.	5.5	48
56	Synthesis of zeolites Na-A and Na-X from tablet compressed and calcinated coal fly ash. Royal Society Open Science, 2017, 4, 170921.	2.4	48
57	Influence of different additives on the synthesis of VO2 polymorphs. Ceramics International, 2013, 39, 8363-8376.	4.8	47
58	Quasi-solid-state fiber-shaped aqueous energy storage devices: recent advances and prospects. Journal of Materials Chemistry A, 2020, 8, 6406-6433.	10.3	47
59	Amorphous manganese silicate anchored on multiwalled carbon nanotubes with enhanced electrochemical properties for high performance supercapacitors. Colloids and Surfaces A: Physicochemical and Engineering Aspects, 2018, 548, 158-171.	4.7	45
60	Synthesis and characterization of belt-like VO2(B)@carbon and V2O3@carbon core–shell structured composites. Colloids and Surfaces A: Physicochemical and Engineering Aspects, 2012, 396, 144-152.	4.7	44
61	Encapsulating V2O3 nanorods into carbon core-shell composites with porous structures and large specific surface area for high performance solid-state supercapacitors. Microporous and Mesoporous Materials, 2018, 262, 199-206.	4.4	43
62	Synthesis of amorphous carbon coated on V2O3 core-shell composites for enhancing the electrochemical properties of V2O3 as supercapacitor electrode. Colloids and Surfaces A: Physicochemical and Engineering Aspects, 2017, 518, 188-196.	4.7	42
63	Fabrication and catalytic activity of ultra-long V2O5 nanowires on the thermal decomposition of ammonium perchlorate. Ceramics International, 2014, 40, 11393-11398.	4.8	41
64	Metal oxide decorated layered silicate magadiite for enhanced properties: insight from ZnO and CuO decoration. Dalton Transactions, 2017, 46, 4303-4316.	3.3	41
65	Synthesis, structure, optical and magnetic properties of interlamellar decoration of magadiite using vanadium oxide species. Microporous and Mesoporous Materials, 2017, 244, 264-277.	4.4	41
66	Engineering Interlayer Space of Vanadium Oxide by Pyridinesulfonic Acid-Assisted Intercalation of Polypyrrole Enables Enhanced Aqueous Zinc-Ion Storage. ACS Applied Materials & Interfaces, 2021, 13, 61154-61165.	8.0	40
67	Polypyrrole-intercalation tuning lamellar structure of V2O5·nH2O boosts fast zinc-ion kinetics for aqueous zinc-ion battery. Journal of Power Sources, 2022, 536, 231489.	7.8	40
68	Mn2+ as the "spearhead―preventing the trap of Zn2+ in layered Mn2+ inserted hydrated vanadium pentoxide enables high rate capacity. Journal of Colloid and Interface Science, 2021, 602, 14-22.	9.4	39
69	Synthesis of bimetallic–organic framework Cu/Co-BTC and the improved performance of thiophene adsorption. RSC Advances, 2019, 9, 15642-15647.	3.6	38
70	Bamboo Leaves as Sustainable Sources for the Preparation of Amorphous Carbon/Iron Silicate Anode and Nickel–Cobalt Silicate Cathode Materials for Hybrid Supercapacitors. ACS Applied Energy Materials, 2021, 4, 9328-9340.	5.1	38
71	Facile synthesis, phase transition, optical switching and oxidation resistance properties of belt-like VO2(A) and VO2(M) with a rectangular cross section. Materials Research Bulletin, 2012, 47, 1978-1986.	5.2	37
72	VO <sub>2</sub> (B) conversion to VO <sub>2</sub> (A) and VO <sub>2</sub> (M) and their oxidation resistance and optical switching properties. Materials Science-Poland, 2016, 34, 169-176.	1.0	37

#	Article	IF	CITATIONS
73	Improvement of the specific capacitance of V2O5 nanobelts as supercapacitor electrode by tungsten doping. Materials Chemistry and Physics, 2017, 186, 5-10.	4.0	37
74	Facile hydrothermal synthesis and electrochemical properties of (NH4)2V6O16 nanobelts for aqueous rechargeable zinc ion batteries. Colloids and Surfaces A: Physicochemical and Engineering Aspects, 2020, 593, 124621.	4.7	37
75	One-step hydrothermal conversion of VO2(B) into W-doped VO2(M) and its phase transition and optical switching properties. Solid State Communications, 2014, 180, 24-27.	1.9	36
76	Facile template-free fabrication of hierarchical V2O5 hollow spheres with excellent charge storage performance for symmetric and hybrid supercapacitor devices. Journal of Alloys and Compounds, 2018, 763, 180-191.	5.5	35
77	Adsorption desulfurization of model gasoline by metal–organic framework Ni3(BTC)2. Journal of Energy Chemistry, 2019, 32, 8-14.	12.9	35
78	A novel route to fabricate belt-like VO2(M)@C core-shell structured composite and its phase transition properties. Materials Letters, 2012, 71, 127-130.	2.6	34
79	Synthesis and characterization of Mn-Silicalite-1 by the hydrothermal conversion of Mn-magadiite under the neutral condition and its catalytic performance on selective oxidation of styrene. Microporous and Mesoporous Materials, 2018, 268, 16-24.	4.4	34
80	Facile synthesis and characterization of LiV 3 O 8 with sheet-like morphology for high-performance supercapacitors. Materials Letters, 2016, 171, 240-243.	2.6	33
81	Facile synthesis of high-surface vanadium nitride/vanadium sesquioxide/amorphous carbon composite with porous structures as electrode materials for high performance symmetric supercapacitors. Applied Surface Science, 2019, 471, 842-851.	6.1	33
82	A dual-polymer strategy boosts hydrated vanadium oxide for ammonium-ion storage. Journal of Colloid and Interface Science, 2022, 606, 1322-1332.	9.4	33
83	"Threeâ€inâ€One―Strategy that Ensures V <sub>2</sub> O <sub>5</sub> Â <i>n</i> H <sub>2</sub> O with Superior Zn <sup>2+</sup> Storage by Simultaneous Protonated Polyaniline Intercalation and Encapsulation. Small Structures, 2022, 3, .	12.0	33
84	Synthesis of V O2(A) nanobelts by the transformation of V O2(B) under the hydrothermal treatment and its optical switching properties. Solid State Communications, 2012, 152, 253-256.	1.9	32
85	Synthesis and characterization of addition-type silicone rubbers (ASR) using a novel cross linking agent PH prepared by vinyl-POSS and PMHS. Polymer Degradation and Stability, 2013, 98, 916-925.	5.8	32
86	Belt-like VO2(M) with a rectangular cross section: A new route to prepare, the phase transition and the optical switching properties. Current Applied Physics, 2012, 12, 875-879.	2.4	31
87	Synthesis of amorphous MnSiO3/graphene oxide with excellent electrochemical performance as supercapacitor electrode. Colloids and Surfaces A: Physicochemical and Engineering Aspects, 2019, 562, 93-100.	4.7	31
88	Hydrothermal synthesis of VO2(A) nanobelts and their phase transition and optical switching properties. Micro and Nano Letters, 2011, 6, 888.	1.3	30
89	Facile one-pot hydrothermal synthesis of belt-like β-V6O13 with rectangular cross sections for Li-ion battery application. Materials Letters, 2015, 160, 404-407.	2.6	30
90	Synthesis of urchin-like Ni3Si2O5(OH)4 hierarchical hollow spheres/GO composite with enhanced electrochemical properties for high-performance hybrid supercapacitors. Dalton Transactions, 2019, 48, 11749-11762.	3.3	30

#	Article	IF	CITATIONS
91	Controlled synthesis and electrochemical properties of vanadium oxides with different nanostructures. Bulletin of Materials Science, 2012, 35, 369-376.	1.7	27
92	Hydrothermal synthesis and electrochemical properties of hierarchical vanadyl hydroxide spheres with hollow core and mesoporous shell. Microporous and Mesoporous Materials, 2017, 249, 137-145.	4.4	27
93	Manganese Silicate Nanosheets for Quasi-Solid-State Hybrid Supercapacitors. ACS Applied Nano Materials, 2021, 4, 8173-8183.	5.0	27
94	Nickel oxide nanoparticles dispersed on biomass–derived amorphous carbon/cobalt silicate support accelerate the oxygen evolution reaction. Journal of Colloid and Interface Science, 2022, 616, 476-487.	9.4	27
95	Direct fabrication of organic carbon coated VO2(B) (VO2(B)@C) core–shell structured nanobelts by one step hydrothermal route and its formation mechanism. Applied Surface Science, 2012, 263, 124-131.	6.1	26
96	One-step hydrothermal synthesis and characterization of V–Cr–O nanospheres and their excellent performance in the ammoxidation of 3,4- and 2,6-DCT. Materials Research Bulletin, 2013, 48, 3620-3624.	5.2	26
97	Ammonia-etching-assisted nanotailoring of manganese silicate boosts faradaic capacity for high-performance hybrid supercapacitors. Sustainable Energy and Fuels, 2020, 4, 2220-2228.	4.9	26
98	Fabrication of belt-like VO2(M)@C core-shell structured composite to improve the electrochemical properties of VO2(M). Current Applied Physics, 2013, 13, 47-52.	2.4	25
99	In situ preparation and optical properties of metal-8-hydroxyquinoline decoration of layered silicate: Self-assembly in the magadiite interface by solid-solid reaction. Microporous and Mesoporous Materials, 2017, 246, 102-113.	4.4	24
100	A facile hydrothermal synthesis of tungsten doped monoclinic vanadium dioxide with B phase for supercapacitor electrode with pseudocapacitance. Materials Letters, 2016, 182, 285-288.	2.6	23
101	Hydrothermal synthesis and supercapacitor electrode of low crystallinity VOOH hollow spheres with pseudocapacitance in aqueous solution. Materials Letters, 2017, 205, 1-5.	2.6	23
102	Fe3O4 nanoparticles/polymer immobilized on silicate platelets for crude oil recovery. Microporous and Mesoporous Materials, 2019, 278, 185-194.	4.4	23
103	Sandwich-Like Sulfur-Doped V2O5/Reduced graphene Oxide/Sulfur-Doped V2O5 Core-shell structure boosts Zinc-Ion storage. Applied Surface Science, 2021, 568, 150919.	6.1	23
104	Dual intercalation of inorganics–organics for synergistically tuning the layer spacing of V <sub>2</sub> O <sub>5</sub> · <i>n</i> H <sub>2</sub> O to boost Zn <sup>2+</sup> storage for aqueous zinc-ion batteries. Nanoscale, 2022, 14, 8776-8788.	5.6	22
105	Template-free synthesis of porous V2O5 flakes as a battery-type electrode material with high capacity for supercapacitors. Colloids and Surfaces A: Physicochemical and Engineering Aspects, 2018, 553, 317-326.	4.7	21
106	A novel intercalation pseudocapacitive electrode material: VO(OH)2/CNT composite with cross-linked structure for high performance flexible symmetric supercapacitors. Applied Surface Science, 2019, 492, 746-755.	6.1	21
107	Self-assembled HVxOy nanobelts/rGO nanocomposite with an ultrahigh specific capacitance: Synthesis and promising applications in supercapacitors. Applied Surface Science, 2019, 481, 59-68.	6.1	21
108	Preparation of V2O3 nanopowders by supercritical fluid reduction. Journal of Supercritical Fluids, 2011, 56, 194-200.	3.2	20

#	Article	IF	CITATIONS
109	Intercalation and in situ formation of coordination compounds with ligand 8-hydroxyquinoline-5-sulfonic acid in the interlayer space of layered silicate magadiite by solid-solid reactions. Microporous and Mesoporous Materials, 2018, 266, 14-23.	4.4	20
110	Facile synthesis of V2O3/C composite and the effect of V2O3 and V2O3/C on decomposition of ammonium perchlorate. Micro and Nano Letters, 2012, 7, 782.	1.3	19
111	Synthesis of Co2SiO4/Ni(OH)2 core–shell structure as the supercapacitor electrode material with enhanced electrochemical properties. Materials Letters, 2021, 282, 128774.	2.6	19
112	Dispersed FeO nanoparticles decorated with Co2SiO4 hollow spheres for enhanced oxygen evolution reaction. Journal of Colloid and Interface Science, 2022, 611, 235-245.	9.4	19
113	Facile synthesis and characterization of rough surface \$\$mathrm{V}_{2}hbox {O}_{5}\$\$ V 2 O 5 nanomaterials for pseudo-supercapacitor electrode material with high capacitance. Bulletin of Materials Science, 2017, 40, 1137-1149.	1.7	18
114	Fabrication of 3D hierarchical porous VO2(B)/CNT/rGO ternary nanocomposite with sandwich-like structure as enhanced electrodes for high-performance supercapacitors. Colloids and Surfaces A: Physicochemical and Engineering Aspects, 2020, 586, 124222.	4.7	17
115	PVA-assisted hydrated vanadium pentoxide/reduced graphene oxide films for excellent Li+ and Zn2+ storage properties. Journal of Materials Science and Technology, 2021, 83, 7-17.	10.7	17
116	Cobalt oxide decorated three-dimensional amorphous carbon/cobalt silicate composite derived from bamboo leaves enables the enhanced oxygen evolution reaction. Chemical Engineering Science, 2022, 251, 117490.	3.8	17
117	Fabrication of V2O3/C core–shell structured composite and VC nanobelts by the thermal treatment of VO2/C composite. Applied Surface Science, 2012, 258, 9650-9655.	6.1	16
118	Changes of medium-range structure in the course of crystallization of zeolite omega from magadiite. Microporous and Mesoporous Materials, 2014, 200, 86-91.	4.4	16
119	A novel route for synthesis and growth formation of metal oxides microspheres: Insights from V 2 O 3 microspheres. Materials Chemistry and Physics, 2016, 177, 543-553.	4.0	16
120	RGO/Manganese Silicate/MOF-derived carbon Double-Sandwich-Like structure as the cathode material for aqueous rechargeable Zn-ion batteries. Journal of Colloid and Interface Science, 2022, 610, 805-817.	9.4	16
121	Controlled synthesis of V <sub>6</sub> O <sub>13</sub> nanobelts by a facile one-pot hydrothermal process and their effect on thermal decomposition of ammonium perchlorate. Materials Express, 2015, 5, 105-112.	0.5	15
122	Changes of medium-range structure in the course of crystallization of mordenite from diatomite. Microporous and Mesoporous Materials, 2015, 206, 52-57.	4.4	15
123	Study on the synthesis of MFI and FER in the presence of n-butylamine and the property of n-butylamine in a confined region of zeolites. RSC Advances, 2016, 6, 114808-114817.	3.6	15
124	Exploring a novel approach to fabricate vanadium carbide encapsulated into carbon nanotube (VC@C) with large specific surface area. Bulletin of Materials Science, 2013, 36, 345-351.	1.7	14
125	Synthesis of zeolite Y from diatomite and its modification by dimethylglyoxime for the removal of Ni(II) from aqueous solution. Journal of Sol-Gel Science and Technology, 2016, 80, 215-225.	2.4	14
126	PVP-assisted hydrothermal synthesis of VO(OH)2 nanorods for supercapacitor electrode with excellent pseudocapacitance. Materials Letters, 2018, 227, 217-220.	2.6	14

#	Article	IF	CITATIONS
127	Synthesis and characterization of hollow V <sub>2</sub> O <sub>5</sub> microspheres for supercapacitor electrode with pseudocapacitance. Materials Science-Poland, 2017, 35, 188-196.	1.0	13
128	Layered silicate magadiite–derived three-dimensional honeycomb-like cobalt–nickel silicates as excellent cathode for hybrid supercapacitors. Materials Today Chemistry, 2021, 22, 100550.	3.5	13
129	Fabrication and electrochemical properties of manganese dioxide coated on cobalt silicate nanobelts core-shell composites for hybrid supercapacitors. Colloids and Surfaces A: Physicochemical and Engineering Aspects, 2020, 600, 124951.	4.7	12
130	Synthesis of V2O3/C composites with different morphologies by a facile route and phase transition properties of the compounds. Materials Science-Poland, 2014, 32, 236-242.	1.0	11
131	Structural regulation of vanadium oxide by poly(3,4-ethylenedioxithiophene) intercalation for ammonium-ion supercapacitors. , 2022, 1, 100013.		11
132	Hydrothermal treatment with VO <sub>2</sub> (B) nanobelts for synthesis of VO <sub>2</sub> (A) and W doped VO <sub>2</sub> (M) nanobelts. Materials Research Innovations, 2015, 19, 295-302.	2.3	10
133	Study on the synthesis of FER and SOD in the presence of ethylene glycol and the oxidation transformation of ethylene glycol in a confined region of zeolites. Journal of Alloys and Compounds, 2017, 696, 788-794.	5.5	10
134	Designed Synthesis and Supercapacitor Electrode of V <sub>2</sub> O <sub>3</sub> @C Coreâ€shell Structured Nanorods with Excellent Pseudoâ€capacitance in Na <sub>2</sub> SO <sub>4</sub> Neutral Electrolyte. ChemistrySelect, 2018, 3, 1577-1584.	1.5	10
135	The synthesis and electrochemical properties of low-crystallinity iron silicate derived from reed leaves as a supercapacitor electrode material. Dalton Transactions, 2021, 50, 8917-8926.	3.3	10
136	Synthesis and electrochemical properties of V2O5nH2O compound with reduced graphene oxide/polyvinyl alcohol film as the free-standing cathode for coin-typed aqueous Zn-ion batteries. Colloids and Surfaces A: Physicochemical and Engineering Aspects, 2021, 613, 126087.	4.7	10
137	Study on the oxidation transformation of hexamethyleneimine in a confined region of zeolites. Microporous and Mesoporous Materials, 2017, 244, 158-163.	4.4	9
138	Self-assembled intercalation of 8-hydroxyquinoline into metal ions exchanged magadiites via solid-solid reaction and their optical properties. Applied Clay Science, 2019, 174, 47-56.	5.2	9
139	Three-Dimensional Network of Vanadium Oxyhydroxide Nanowires Hybridize with Carbonaceous Materials with Enhanced Electrochemical Performance for Supercapacitor. ACS Applied Energy Materials, 0, , .	5.1	8
140	High pH promoting the synthesis of V-Silicalite-1 with high vanadium content in the framework and its catalytic performance in selective oxidation of styrene. Dalton Transactions, 2018, 47, 11375-11385.	3.3	8
141	Rice-like and rose-like zinc silicates anchored on amorphous carbon derived from natural reed leaves for high-performance supercapacitors. Dalton Transactions, 2021, 50, 9438-9449.	3.3	8
142	Active Functional Group-coated VO2(B) Nanorods: Facile One-pot Hydrothermal Synthesis and Conversion to V2O3. Chemistry Letters, 2014, 43, 337-339.	1.3	7
143	Intercalation of calcein into layered silicate magadiite and their optical properties. Royal Society Open Science, 2017, 4, 171258.	2.4	7
144	Facile hydrothermal synthesis and electrochemical properties of (NH4)2V4O9 sheets for supercapacitor electrode with excellent performance. Materials Letters, 2018, 229, 26-30.	2.6	7

#	Article	IF	CITATIONS
145	The influence of VO2(B) nanobelts on thermal decomposition of ammonium perchlorate. Materials Science-Poland, 2015, 33, 560-565.	1.0	6
146	Study on the oxidation transformation of diethylamine in a confined region of ZSM-22. Materials Letters, 2017, 206, 84-86.	2.6	5
147	Influence of the electrochemical properties of vanadium oxides on specific capacitance by molybdenum doping. Bulletin of Materials Science, 2019, 42, 1.	1.7	5
148	Synthesis and characterization of VO <sub>2</sub> @poly(sodium styrene sulfonate)/polypyrrole using VO <sub>2</sub> @PSS as a template. Materials Express, 2015, 5, 351-358.	0.5	4
149	Cobalt silicate: critical synthetic conditions affect its electrochemical properties for energy storage and conversion. Dalton Transactions, 2022, 51, 2815-2826.	3.3	4
150	In-situ synthesis of V2O5 hollow spheres coated Ni-foam as binder-free electrode for high-performance symmetrical supercapacitor. Materials Letters, 2019, 248, 101-104.	2.6	3
151	Synthesis and phase transition properties of VO 2 (M) hollow spheres with large thermal hysteresis width. Micro and Nano Letters, 2019, 14, 819-822.	1.3	3
152	Rapid Combustion Synthesis of Metal Oxides Species Highly Dispersed on Layered Silicate Magadiite. ChemistrySelect, 2020, 5, 569-574.	1.5	3
153	Fabrication of Phosphorus-Doped Cobalt Silicate with Improved Electrochemical Properties. Molecules, 2021, 26, 6240.	3.8	3
154	Hierarchical VOOH hollow spheres for symmetrical and asymmetrical supercapacitor devices. Royal Society Open Science, 2018, 5, 171768.	2.4	2
155	Formation and optical properties of metal/10-hydroxybenzo[h]quinolone complexes in the interlayer spaces of magadiite by solid–solid reactions. Royal Society Open Science, 2018, 5, 171732.	2.4	2
156	Preparation of Amorphous Carbon Nanotubes (a-CNTs) from Vanadium Dioxide@Organic Carbon Core–Shell-structured Composites and Their Thermal Stability in Air. Chemistry Letters, 2013, 42, 1502-1504.	1.3	1